Journal of Engineering Mathematics, Vol. 8, No. 3, July 1974
Noordhoff International Publishing–Leyden
Printed in The Netherlands

Numerical studies for viscous swirling flow through annular diffusers

Part II. Results

C. M. CRANE

School of Mathematics, Computing and Statistics, City of Leicester Polytechnic, Leicester, England.

D. M. BURLEY

Department of Applied Mathematics and Computing Science, University of Sheffield, Sheffield, England

(Received September 25, 1974)

SUMMARY

Numerical solutions (obtained using the method of Part I) for incompressible viscous swirling flows through annular diffusers are discussed. Separation of the boundary layer and vortex breakdown are predicted. The prime interest is devoted to investigating the type of separation and the effects on separation of inlet swirl and Reynolds number. Pressure distributions have been calculated and performance parameters evaluated. The effect of separation on performance is also clearly shown.

1. Introduction

In practice, most diffusers operate under turbulent flow conditions. Many experimental studies have been made for the more simple geometries (particularly straight walled two-dimensional diffusers) and much has been achieved in the understanding of the basic flow features. The work here is based on the laminar flow model set up in Part I, [1], of this series of papers and the notation and diagrams will be used without explanation. The approach used does allow more detailed study of separation and flow recirculation than is possible with the well established boundary layer techniques. Turbulence modelling is achieving a high degree of sophistication and it is thought that an extension of the present method to include turbulent flows is now feasible.

Four different flow régimes have been observed in experimental studies of diffuser flow behaviour of which three have steady or reasonably steady flow. For two-dimensional diffusers, charts have been prepared [2], [3] from experimental data defining lines separating these régimes on a diffuser angle *versus* diffuser length graph. The dividing lines do not represent sharp transitions and their definition involves a certain amount of arbitrariness and subjectivity. Complete charts for annular and conical units do not seem to be available though it is suggested on the basis of the experiments that have been performed, that they would be very similar. Of course, diffuser angle and length are not the only factors affecting the flow régime. Inlet boundary layer thickness and velocity profile, for example, also have a large influence [4].

For annular and conical units, the important case of swirling flows can be considered. In practice, swirling flows in diffusers are very common, for example, behind blade rows of turbines and compressors. It has been demonstrated experimentally ([5], [6], [7]) and predicted numerically ([8], [9]) that swirl can cause separation and vortex breakdown, both of which are detrimental to performance. However, experimental evidence suggests that in diffusers, certain swirl conditions can in fact lead to improved performance ([10], [11]).

For the class of diffusers under study, among the many parameters that may be varied are: Reynolds number, diffuser angle, diffuser length, inlet swirl velocity profile, inlet radial velocity profile, hub diameter, hub rotation and exit boundary conditions. The convergence of the computational method is relatively slow, and to investigate fully the effects of all the above

parameters would require a prohibitive amount of computer time. Most of the work has therefore been centered on a single geometry with a fixed inlet radial profile for different swirl conditions and a range of Reynolds numbers ($0 < R \leqq 2500$). For all the computations reported here, the transverse velocity, V_θ, has been taken as zero at inlet.

Experimental results for a diffuser of similar geometry to those considered here have been obtained by Hoadley in [10]. The work consists of measuring the pressure and velocity componets in the diffuser at a single Reynolds number for three inlet swirl conditions. The present theoretical results cannot be compared directly with these experimental results for the following reasons:

(i) the Reynolds number of the flow was extremely high $\sim 10^6$,
(ii) the flow had turbulent boundary layers, and
(iii) the exit boundary conditions in the experiments differ considerably from those used here. Hoadley's apparatus was fitted with a converging section at the diffuser exit which tends to inhibit separation and in fact promotes reattachment for already separated flows.

However, the inlet radial velocity profile (curve (a) of fig. 1) and some of the inlet swirl profiles of this study (curves (1), (4) and (5) of fig. 1) are taken from Hoadley's data.

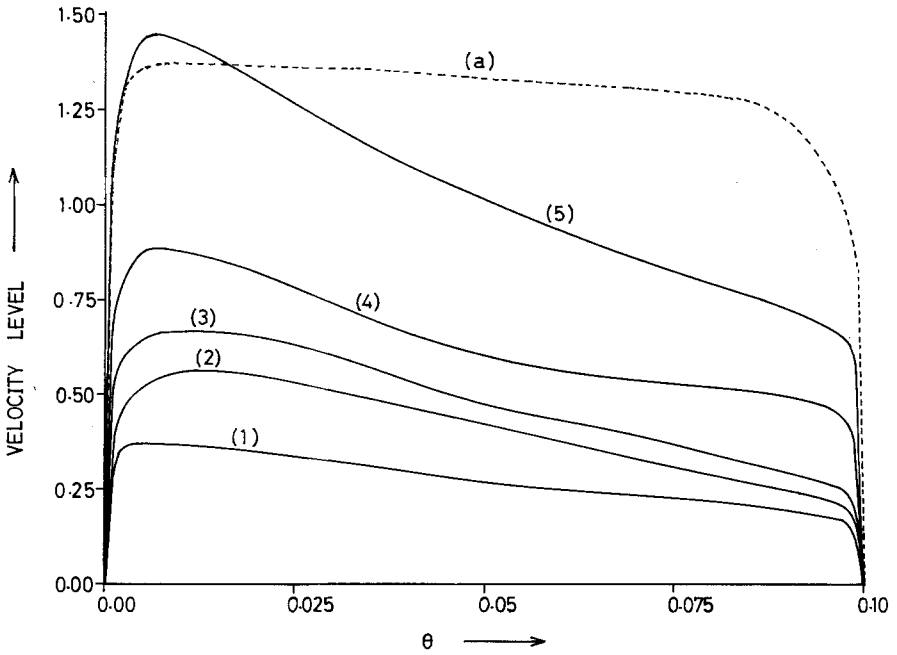

Figure 1. Inlet velocity profiles. Curve (a) is the radial velocity profile and curves (1)–(5) are the swirl velocity profiles.

The non-dimensionalisation of the inlet velocities is taken to be the same as that used by Hoadley. He non-dimensionalised with respect to a typical velocity of 50 ft./sec. and this leads to an average inlet radial velocity (direction r) of 1.265. This, of course, results in a rather lower Reynolds number than a more usual non-dimensionalisation would give. The inlet swirl profiles (1), (4) and (5) of fig. 1 correspond to swirl blade angles of 10°, 20° and 30° in Hoadley's experiments.

1.1. *Diffuser dimensions*

Most of the present results have been obtained for a diffuser having in the notation of [1]:

(i) an outer casing angle of $\theta = 0.1$ radians,
(ii) a cylindrical hub with radius $R = 0.5$,

(iii) an inlet specified by $r=10.0$ so that R at inlet at the outer casing is given by $R\doteq 1.5$,
(iv) an exit specified by $r=20.0$ so that R at exit is given by $R\doteq 2.5$.

The area ratio is then almost exactly 3. A number of results have been obtained for different angles and lengths. In all cases r_{inlet} is varied so that the inlet area is kept constant with the same mass flow rate of fluid into the diffuser. Unless otherwise specified, however, the dimensions of the diffuser will be assumed as specified in (i)–(iv) above.

In the discussion of the results, three different types of pressure will be mentioned.

(i) *Static pressure.* This is often called simply the pressure and was denoted by P in part I.
(ii) *Stagnation pressure.* This is sometimes called the total pressure. In part I it was denoted H and in non-dimensional terms is related to P by $H=P+\frac{1}{2}V^2$.
(iii) *Dynamic pressure.* This is the difference between stagnation and static pressure i.e.

$$\text{Dynamic pressure}=H-P=\tfrac{1}{2}V^2 .$$

2. Flow regimes and separation

2.1. *Separation: definitions and detection*

Difficulties are involved in the definition of separation since in three dimensions, separation can occur without the usual flow reversal and reduction of the wall shear stress to zero. Two-dimensional definitions of separation which usually depend on these factors are useless for three-dimensional flow. Although the flow under consideration here is axially symmetric and hence essentially two-dimensional, the presence of swirl gives a three-dimensional character to the boundary layer. A rigorous and more general definition of separation that is meaningful in three dimensions has been developed in [12] and subsequently reported in more readily accessible literature [13]. A point where a limiting stream-line leaves a surface is called a separation point. Within this context there are two types of separation called ordinary and singular. For singular points there is no shear at the wall and the inclination of the limiting streamline in a plane perpendicular to the wall is indeterminate. At ordinary points, on the other hand, there is a shear stress component in the plane of the wall and the limiting streamline is therefore tangential to the wall. In terms of the present situation

$$\tan T_0 = \lim_{\theta\to 0}\frac{\partial V_\theta/\partial\theta}{\partial q/\partial\theta} = \begin{cases} 0 \text{ at ordinary points} \\ \text{indeterminate at singular points} \end{cases} \tag{2.1}$$

where T_0 is the inclination of the limiting streamline to the wall at the point of separation and $q^2=V_\theta^2+V_r^2$.

With the present axially symmetric model $\partial V_r/\partial\theta=0$ at a separation point. Since $\partial V_\theta/\partial r$ is very small in the boundary layer and in fact zero on the boundary, it follows that ξ, and hence Ω, must vanish at a separation point. The criterion used for detection of a separation point was therefore a change in sign of the wall vorticity. The validity of the criterion was verified by separation of the limiting streamline, but in general, tests based on the stream function proved much less sensitive.

2.2. *The types of separation predicted.*

Investigation of the shear stresses in the plane of the wall at separation enables the type of separation to be determined. It should perhaps be mentioned that at the boundary itself, $V_\theta\equiv 0$ and by continuity,

$$\lim_{\theta\to\theta_{\text{boundary}}}\frac{\partial V_\theta}{\partial\theta}=0 . \tag{2.2}$$

The shear stress normal to the wall must therefore be zero. Since at separation $\partial V_r/\partial\theta$ is also zero, it follows from (2.1) that separation is singular or ordinary according as $\partial V_\theta/\partial\theta$ is zero or

non-zero. Thus in the absence of swirl, the separation will automatically be singular. Detailed examination of the swirl velocity profiles at the location of separation shows them to be almost exactly linear so that there is a non-zero azimuthal shear stress. Separation in the presence of swirl is therefore usually ordinary. However, it does seem possible that under certain freak combinations of inlet swirl and hub/wall rotation, $\partial V_\theta/\partial\theta$ could be made to vanish at separation. This, of course, would result in a singular separation line.

In spite of the assumption of axial symmetry, the presence of swirl gives a three-dimensional character to the boundary layer (it becomes skewed). The limiting streamlines in the plane of the wall meet in a cusp which defines the separation line (i.e. a circle of constant r on the boundary). In practical situations, ordinary separation is the usual type encountered, but points of singular separation do occur. Lines of singular separation, however, have never been observed though there is no theoretical reason why they should not exist. It seems likely that a line of singular separation would constitute a highly unstable configuration.

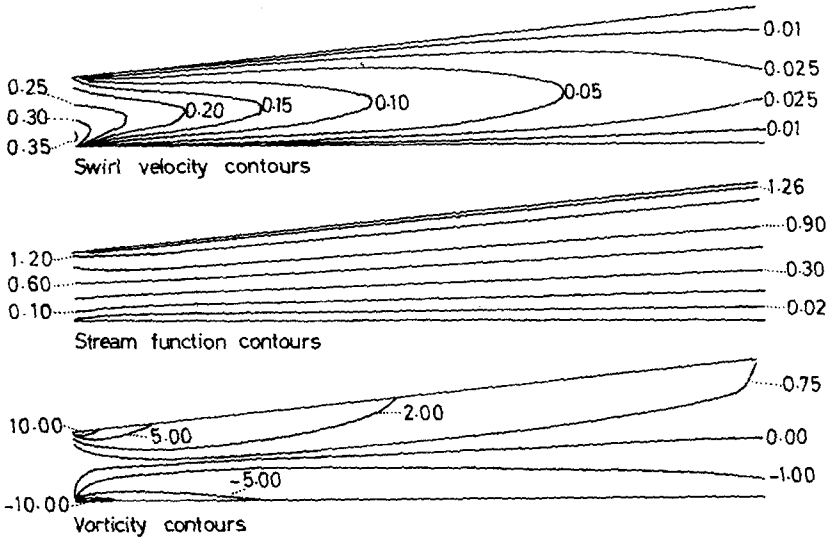

Figure 2. Contours for Reynolds number 25 and inlet swirl profile (1).

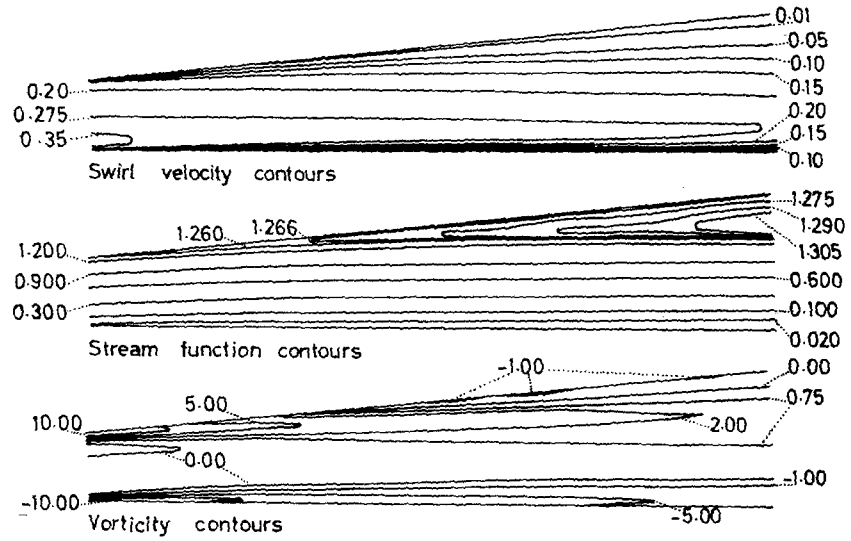

Figure 3. Contours for Reynolds number 2000 and inlet swirl profile (1).

2.3. *The flow régimes*

In the absence of swirl, four basic flow régimes have been observed [11] for two dimensional diffusers. These are:

(i) *No appreciable stall régime* where at most small regions of separation are observed.

(ii) *Large transitory stall régime* characterised by gross fluctuations of the whole flow pattern. Relatively large separated regions form and are then washed out of the diffuser. Since the flow is unsteady, this régime cannot be predicted using the present steady-state flow model.

(iii) *Fully developed stall régime* where the flow is essentially steady and separated from one wall.

(iv) *Jet flow régime* where separation occurs very near the inlet or throat of the diffuser from both walls. Again this is a relatively steady flow.

For swirling flows in conical diffusers a fifth régime in the form of vortex breakdown is possible provided swirl gradients are sufficiently large. Experimental observations have detected

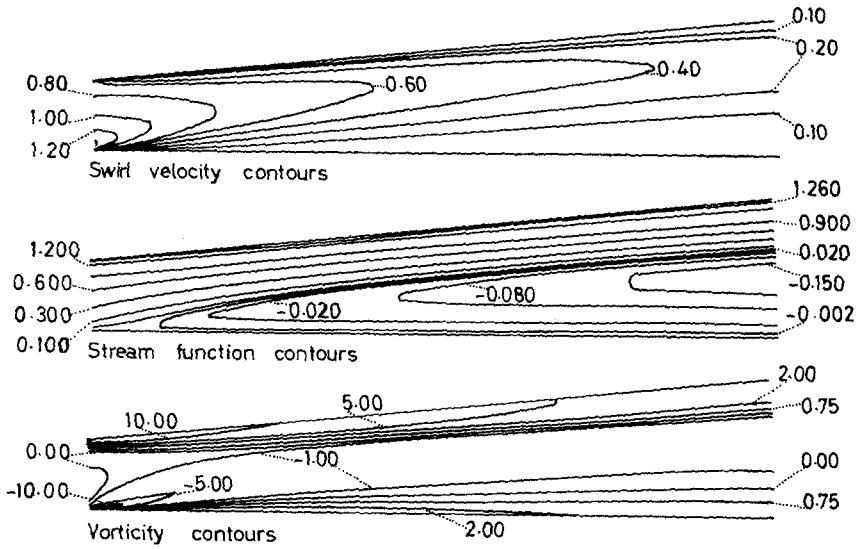

Figure 4. Contours for Reynolds number 200 and inlet swirl profile (5).

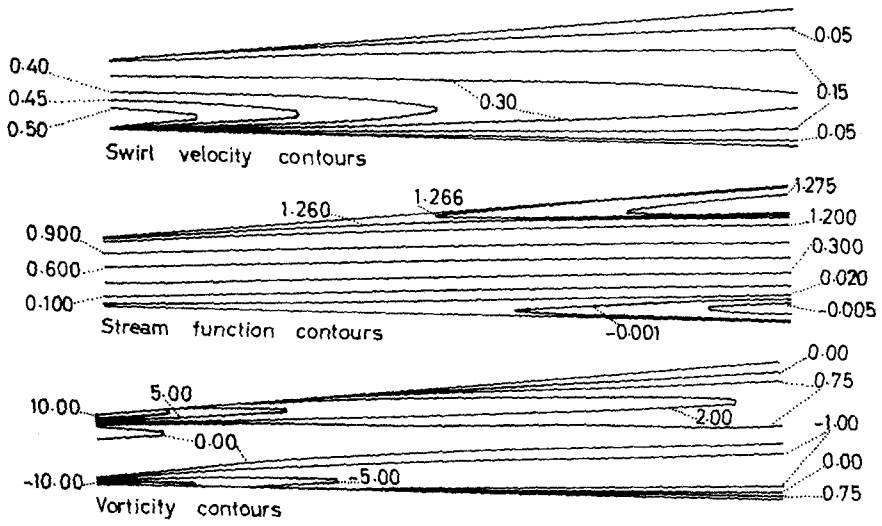

Figure 5. Contours for Reynolds number 1000 and inlet swirl profile (2).

vortex breakdown where a separation bubble forms at the axis (*e.g.* [6], [7] and [11]). With the presence of a hub, this type of vortex breakdown is not possible, but instead, separation from the hub has been observed [10]. The numerical results obtained in the present investigation have indicated (see figs. 2–5) the presence of four flow régimes:

(i) no separation and essentially uniform flow
(ii) separation from the outer wall
(iii) separation from the hub, and
(iv) separation from the hub and outer wall simultaneously. The contour plots have been obtained using [14]

3. Factors influencing separation

Some of the effects of Reynolds number and swirl on separation are shown for a fixed geometry in figs. 6–9. It can be seen that in general, for any given inlet swirl profile, the larger the Reynolds number, the more extensive the separation.

(a) *No swirl.* Separation occurs from the outer casing only and onset of separation extends further and further upstream with increasing Reynolds number. The curve for inlet swirl profile (1) is virtually identical to this curve. Any discernable differences indicate marginally earlier

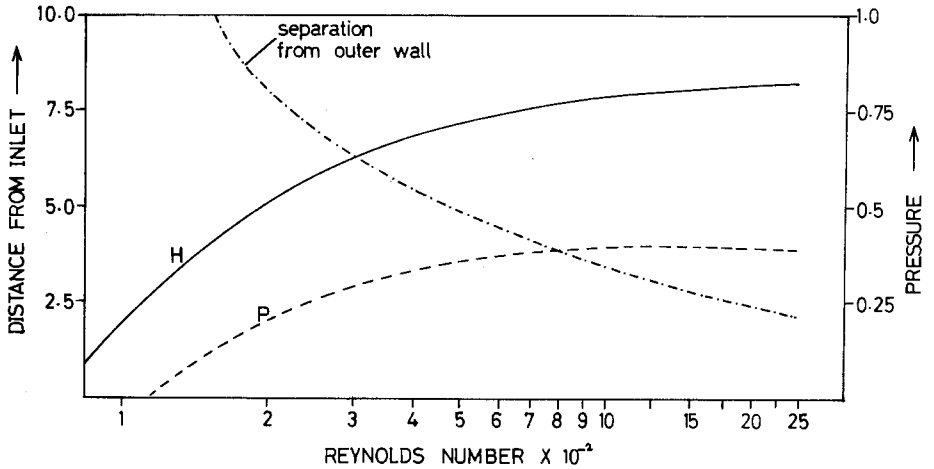

Figure 6. Pressure recovery and location of separation for the case of no swirl (results for inlet swirl profile (1) virtually identical).

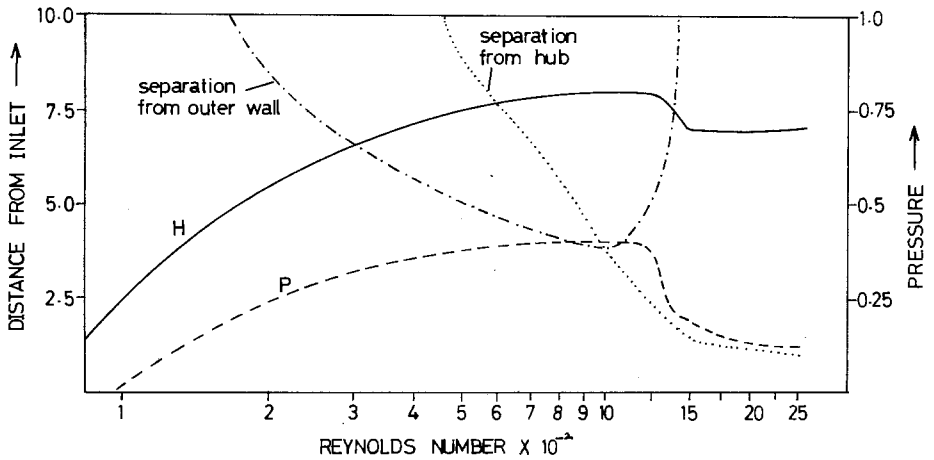

Figure 7. Pressue recovery and location of separation for the case of inlet swirl profile (2).

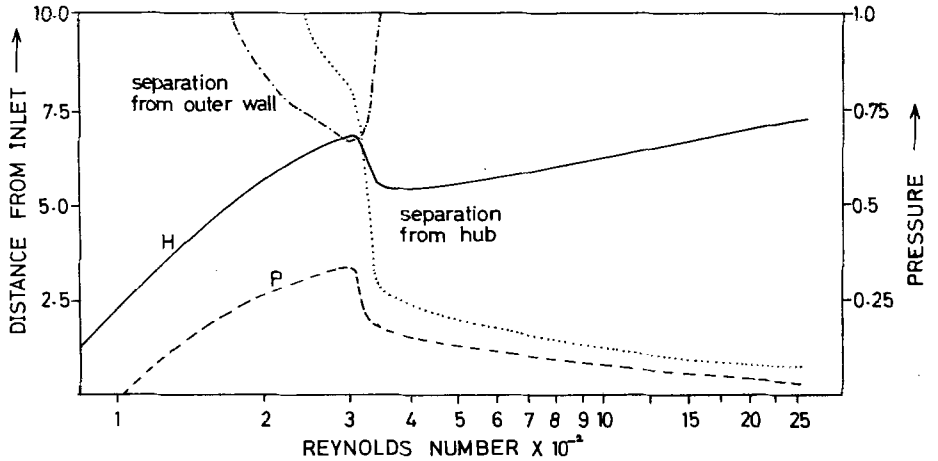

Figure 8. Pressure recovery and location of separation for the case of inlet swirl profile (3).

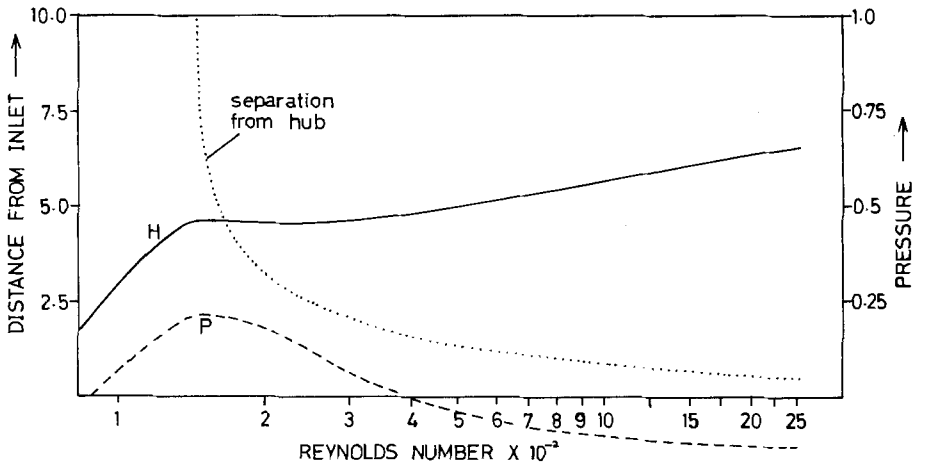

Figure 9. Pressure recovery and location of separation for the case of inlet swirl profile (4).

separation. This is a little surprising since the general effect of inlet swirl is to delay and reduce separation at the outer casing.

(b) *Inlet swirl profile* (2). This is a most interesting case since at certain Reynolds numbers, separation can occur from the outer casing, the hub or both. As can be seen from the diagram, separation from the outer casing occurs first and extends upstream with increasing Reynolds number for $R < 1000$. For Reynolds numbers above 1000, hub separation becomes dominant and the separated region at the outer casing diminishes and quickly disappears.

(c) *Inlet swirl profile* (3). A similar pattern to (b) is displayed but the separation at the outer casing never becomes quite so extensive and the hub separation becomes dominant for $R > 300$.

(d) *Inlet swirl profile* (4). Separation was first detected at the hub for a Reynolds number of 150. As before, increasing the Reynolds number increased the extent of the separation. No separation at the outer casing was observed.

(e) *Inlet swirl profile* (5). The trend of earlier and more dominant hub separation with increasing swirl, was observed to continue. The onset of separation for this case was below $R = 100$ but above $R = 75$. Combining inlet swirl profile (5) with a hub rotation that produces a swirl value of 1.0 at the hub surface results in slightly delayed separation throughout the Reynolds number range.

On the basis of these results for separation, the following comments are particularly relevant:

(i) The numerical procedure predicts separation but the nature of the exit boundary conditions

(similar to free slip radially directed guide vanes at the exit) restricts the type of recirculating region that can occur.

(ii) Increasing the Reynolds number results in more extensive separation. Experiments show that for turbulent flow with $R > 10^4$ any variation in Reynolds number has minimal effect. At very low R, viscous effects are large and in fact a favourable pressure gradient is needed to drive the flow. For this situation, in the absence of swirl, separation will not occur. As the Reynolds number is raised, viscous interactions have less effect and in fact some of the energy lost by the diffusing process is converted to pressure energy and a pressure rise through the diffuser takes place. With further increases in R, the now adverse pressure gradient can become sufficiently strong to drive a reverse flow near the boundaries and hence separation occurs.

(iii) Swirling flows tend to reduce separation at the outer wall but cause separation at the hub. This tendency is linked to the vortex breakdown phenomenon discussed in [9]. It was shown there that strong negative axial swirl gradients can produce reverse flow at the axis. In the present situation, the axis is not included but the tendency is the same. In fact, it is easier to cause separation at the hub than it would be to produce reverse flow at the axis were the hub removed. This is because the dynamic pressure close to the hub surface in the absence of swirl is much smaller than the dynamic pressure at the axis of symmetry would be. In [9] it was found that a smaller swirl ratio was required to cause flow reversal at high R than at low R. This effect is again predicted here since, for cases (2) and (3) of fig. 1, at lower R the swirl is insufficient to cause hub separation whereas at high R not only does hub separation occur, but also, separation at the outer casing is prevented.

(iv) It should be noted that profile (a) of fig. 1 is not fully developed. Therefore, for different R, it will represent a different stage of development. In fact, this means that for higher R, the flow is closer to separation as it enters the diffuser. Hence, there are two reasons for the predicted earlier separation at higher R: firstly, and most fundamentally, viscous losses are smaller making possible a static pressure rise (i.e. an adverse pressure gradient) and secondly, the inlet flow is somewhat closer to the separation condition.

(v) The exit boundary conditions are partly responsible for the steepness of the separation curve when separation occurs close to the exit.

3.1. *Diffuser length (constant angle)*

A number of results have been obtained where the length is altered for a diffuser in which separation has already occurred. These results, recorded in table 1, are for a Reynolds number of 250 and a diffuser angle of 0.1 radians.

TABLE 1

Diffuser length	*Distance from inlet of separation*
7.436	7.23
8.718	7.06
10.000	7.03
11.282	7.02
12.564	7.02
13.846	7.02

These results give some indication of the upstream influence of the exit boundary conditions. If the exit is well past the onset of separation, any additional increase in length has virtually no effect. For a shorter diffuser, but just long enough for separation to occur, separation was delayed slightly. It is the upstream influence of the boundary conditions at exit constraining the flow to be radially directed that is responsible for this delay.

3.2. *Diffuser angle*

The investigation of the variation of separation with diffuser angle was again carried out for R = 250 in the absence of swirl. With increasing angle, as would be expected, the separated regions become more extensive. Convergence also becomes more difficult to achieve as the diffuser angle is increased. For the larger diffuser angles (> 0.3 radians), the normal convergence criterion could not be satisfied (in reasonable computing time) and was relaxed somewhat. In table 2, the distance from the inlet of the location where separation (both at the outer wall and at the hub) was first detected is given.

TABLE 2

R	*Angle in radians*	r_{inlet}	*Outer casing separation*	*Hub separation*
250	0.075	15.0		
250	0.085	11.765	8.39	
250	0.1	10.0	7.03	
250	0.2	5.0	2.37	
250	0.3	3.333	1.42	4.40
250	0.4	2.5	1.0	2.55
250	0.5	2.0	0.75	2.32
250	0.6	1.667	0.66	1.96
250	0.65	1.5395	0.56	1.92

In all cases, the diffuser length was 10 inlet annulus widths. The position of the origin was altered so that the same mass flow rate (to within 1 %) was achieved for each diffuser.

For diffuser angles $\leqq 0.075$ radians no separation at all is detected, but as the angle is increased, separation occurs first at the outer casing. Further increases in diffuser angle result in the separated region spreading further upstream. When the angle exceeds about 0.3 radians, separation also takes place at the hub and the flow takes the form of an annular jet (jet flow régime). For angles in excess of 0.7 radians the computer program failed to give intelligible results.

Results have also been obtained for diffusers having constant area ratio* but different angles (and hence also different lengths) under varying degrees of swirl. This investigation was primarily concerned with the relative efficiencies (see section 5) of the different diffusers but the separation locations are given in table 3.

TABLE 3

Length	*Angle radians*	*Distance from inlet where separation commences*									
		No swirl		*Inlet swirl profile* 1		*Inlet swirl profile* 2		*Inlet swirl profile* 3		*Inlet swirl profile* 4	
		WALL	HUB	WALL	HUB	WALL	HUB	WALL	HUB	WALL	HUB
20.0	0.05	/	/	/	/	/	/	/	/	/	/
16.0	0.0625	14.374	/	14.996	/	/	/	/	/	/	9.939
13.33	0.075	10.28	/	10.55	/	11.01	/	11.47	/	/	5.05
10.0	0.1	7.03	/	6.93**	/	7.240	/	7.341	9.343	/	2.375
8.0	0.125	4.56	/	4.64	/	4.84	/	5.23	5.44	/	1.424
6.67	0.15	3.43	/	3.50	/	3.66	/	/	1.78	?	?

/ indicates "separation not detected"
? indicates "convergence not achieved"
** obtained by interpolation from results for R of 200, 300 and 400.

* area ratio = area of exit annular surface/area of inlet annular surface
= 3 for all these cases.

3.3. *Other factors*

For a Reynolds number of 250, the effects of swirl induced by hub rotation have been investigated. Hub swirl values between 0 and 3.5 were considered. Swirl introduced in this way did not have as profound an effect as inlet swirl. In general it was found that the stronger the hub swirl the earlier the separation: for a hub swirl of 3.5 separation occurred approximately 1 inlet annulus width earlier than in the absence of swirl. Separation at the outer wall boundary only was detected. It should be noticed that for the case of swirl induced solely by hub rotation there is a small positive axial swirl gradient and this tends to accelerate the fluid near the hub and consequently retard that near the casing. Thus the predicted result of slightly earlier separation with increased hub swirl is to be expected.

One very important factor that has not been investigated in great detail is that of variation of inlet radial velocity profile. The fully developed pipe annulus profile has been considered and shown to produce earlier separation [9]. Preliminary results for more non-uniform inlet radial profiles have shown strong effects on separation and the boundary from which it occurs.

4. Physical flow characteristics

Computed results for annular diffuser flows have been obtained for well over two hundred different cases. Presentation and detailed description of all the results is therefore clearly impossible. Brief mention will now be made of some of the more interesting features and general trends. A sample of results is displayed in figs. 10–12, the curves shown corresponding to the cases for which contour plots have been given.

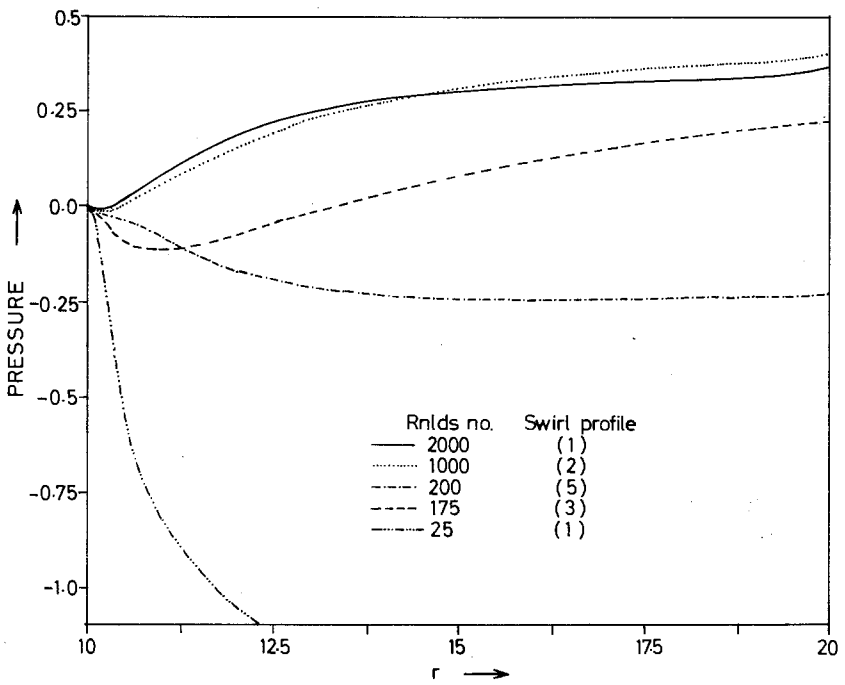

Figure 10. Flux of pressure recovery normalised on inlet dynamic head.

Velocity distribution at exit. For low Reynolds numbers in the absence of strong swirl, the profile is virtually the same shape as the theoretical axial velocity profile for fully developed flow through a pipe annulus. Increasing the Reynolds number or swirl produces pressure gradients that cause distortion of this profile and in fact can result in reverse flow in the region of the outer wall or hub boundaries.

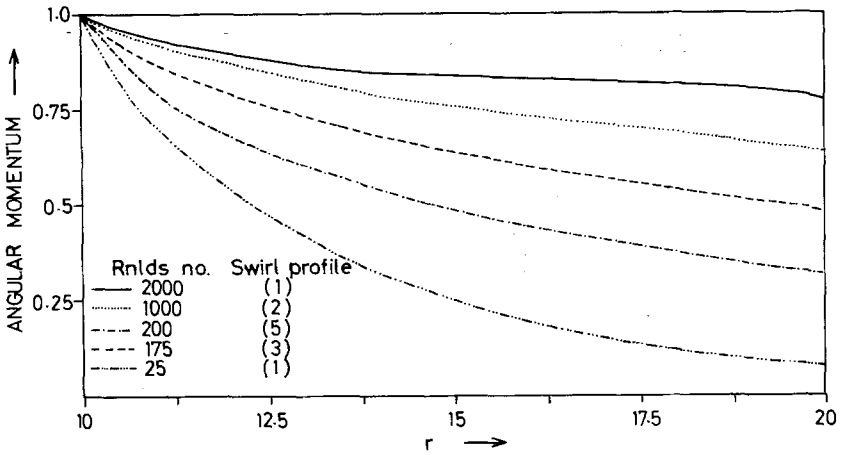

Figure 11. Flux of angular momentum decay normalised on flux of angular momentum at inlet.

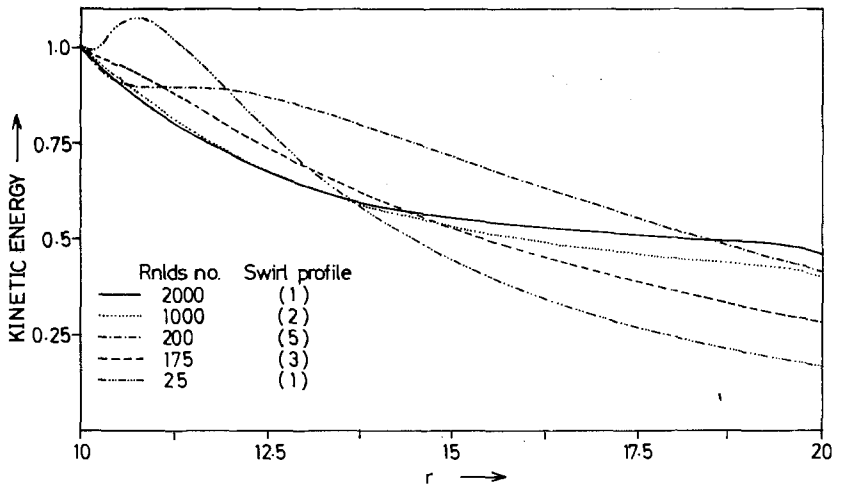

Figure 12. Flux of kinetic energy decay normalised on flux of kinetic energy at inlet.

Pressure recovery. A selection of pressure recovery curves normalised on the inlet dynamic head is given in fig. 10. For low Reynolds numbers, when viscous interactions are large, pressure is lost through the diffuser i.e. a favourable pressure gradient is required throughout the length of the diffuser in order to drive the flow. In all cases, a small pressure loss takes place immediately following the inlet due to the redistribution of the inlet velocity. When pressure recovery is possible, it tails off as the separation condition is approached. Separation at the hub induced by swirl is far more detrimental to pressure recovery than separation at the outer wall.

A small sudden increase in pressure at the exit is apparent and is a result of the exit boundary conditions. At the exit, the flow is constrained to be radially directed and this prevents separation zones from extending, thus increasing the efficiency of the diffusion proces..

Angular momentum decay. Fig. 12 shows some angular momentum decay curves considered from the flux point of view. Swirl momentum is maintained best for high Reynolds numbers and low inlet swirl.

Kinetic energy decay. Reynolds number and swirl both have a marked effect or kinetic energy decay. For low Reynolds numbers it is possible for the kinetic energy to increase in the inlet region. This feature is due to the redistribution of the velocity profile as a result of the thickening boundary layer and is necessarily accompanied by a large pressure drop. The forming of separated regions also reduces kinetic energy decay. Ideally a uniform velocity profile is required so that kinetic energy decay and pressure recovery are both as large as possible.

Pressure profiles. At inlet the pressure is highly non-uniform, especially when the fluid is swirling strongly. Large vorticity values near the boundaries lead to very high pressure gradients in the immediate vicinity of the walls. At exit the pressure is very much more constant even for highly swirling flows. In regions of flow recirculation the pressure is virtually constant and at the walls the pressure gradients are negligible.

5. Pressure recovery coefficients and diffuser effectiveness

In addition to variation of separation point with Reynolds number, figs. 6–9 also show the variation of two quantities C_{HM} and C_{PM} with Reynolds number. C_{PM} is the static pressure recovery coefficient and this gives a measure of inlet kinetic energy recovered as pressure energy. C_{HM} is the normalised total energy recovery or stagnation pressure recovery coefficient. This gives the proportion of inlet kinetic energy retained as kinetic energy plus the proportion converted to pressure energy. Both C_{PM} and C_{HM} have been calculated using mass flow or flux averaging. Investigation of these recovery coefficients reveals the following:

(i) For low R (i.e. when viscous effects are large) the recovery coefficients are negative.

(ii) The difference between the curves at a given R gives the kinetic energy at exit. As the Reynolds number is increased, the difference between these curves increases indicating that more and more kinetic energy is being taken up by the recirculating regions.

(iii) In figs. 7 and 8 a curious feature is observed in that the recovery coefficients take a sudden dip. Comparison with the separation curves reveals that this dip occurs in the Reynolds number range where separation from the outer wall is disappearing and separation from the hub begins to dominate. When hub separation takes over entirely, the cause of the separation is no longer the adverse pressure gradient produced as a result of the expanding flow passage, but the strength of the axial swirl gradient. It is interesting to note that maximum pressure recovery occurs when the outer wall separation starts to reduce.

(iv) For inlet swirls sufficiently strong that separation from the hub only occurs, once the separation has started, increasing the Reynolds number decreases the static pressure recovery coefficient.

From these results it can be seen that separation induced by swirling flows can be highly detrimental. It is worth comparing the trends here with those of the rotating cylindrical pipe studies in [8] and [9]. It was notices there that the swirl ratio required to produce vortex breakdown is lower at high R than at low R. Here, inlet swirl conditions that do not cause separation at the hub for low R (but may allow outer wall separation at low R) can cause large reverse flow regions at the hub for higher R.

5.1. *Ideal pressure recovery coefficient*

The ideal pressure recovery coefficient for one-dimensional flow is given by

$$C_{A_i} = 1-(AR)^{-2} \text{ (where } AR \text{ denotes the area ratio)}$$
$$= 0.889 \text{ for the geometry of the majority}$$

of the present calculations. Using the mass flow averaged formula given in part I for the ideal pressure recovery coefficient (based on the actual inlet flow) gives different values depending on the inlet swirl. These different values are recorded in table 4.

5.2. *Performance comparison for diffusers of equal area ratio*

The recovery coefficients and effectiveness will now be examined for the cases considered in table 3. All the results are for a Reynolds number of 250 and a constant area ratio of 3.0. The values obtained for C_{PM} and E_M are given in table 5.

In general, the inlet swirl increases the pressure recovery coefficient and effectiveness unless the swirl gradient is sufficiently strong to cause substantial separation at the hub. Even for the

TABLE 4

Inlet swirl profile	*Value of* C_{PM_i}
No swirl	0.884
1	0.865
2	0.847
3	0.834
4	0.797
5	0.716

TABLE 5
(R = 250, $AR = 3.0$)

Length	*Angle radians*	*No swirl*		*Inlet swirl ∂rofile* 1		*Inlet swirl profile* 2		*Inlet swirl profile* 3		*Inlet swirl profile* 4	
		C_{PM}	E_M	C_{AM}	E_M	C_{PM}	E_M	C_{AM}	E_M	C_{AM}	E_M
20.0	0.05	0.069	0.078	0.093	0.107	0.124	0.146	0.142	0.170	0.178	0.224
16.0	0.0625	0.139	0.158	0.160	0.185	0.189	0.223	0.206	0.247	0.239	0.300
13.33	0.075	0.185	0.209	0.203	0.235	0.230	0.271	0.246	0.295	0.241	0.302
10.0	0.1	0.253	0.286	0.258	0.298	0.339	0.287	0.300	0.360	0.119	0.148
8.0	0.125	0.280	0.316	0.291	0.337	0.313	0.369	0.329	0.394	0.046	0.058
6.67	0.15	0.305	0.345	0.315	0.364	0.335	0.396	0.206	0.246	?	?

? indicates convergence not achieved

0.5 angle diffuser where no separation was detected, inlet swirl increases the pressure recovery. This is because the swirl causes the boundary layer at the outer wall to be thinned thereby effectively widening the flow passage.

6. Computational details

For most of the calculations a 40×19 mesh has been used with 40 uniformly spaced radial mesh stations and 19 non-uniformly spaced stations in the transverse direction. For the longer diffusers, as many as 60 radial mesh stations have been used.

Obtaining convergence is relatively difficult for this problem. Several factors play a part in determining how easily convergence can be achieved. In general, the higher the Reynolds number and the larger the inlet swirl velocity, the more cycles are required. However, the choice of relaxation parameters and suitability of the initial guess are also vitally important. The initial guess was usually taken as the previous most comparable solution. Typical relaxation parameters used for this problem are 0.45, 0.7 and 1.2 for vorticity, stream function and swirl velocity equations respectively. Depending on the conditions, convergence was normally obtained in somewhere between 100 and 800 iterative cycles. Some cases, however, were particularly stubborn. For example, for a Reynolds number of 350 with inlet swirl profile 3, approximately 2,500 iterative cycles were required. This case correspnds to the change over point where hub separation suddenly takes over entirely.

For most of the calculations, the vorticity boundary weighting parameter, α, was given a value of 0.5. The convergence criterion tolerance, ε, was taken as 5×10^{-3}. Experience shows that when this is satisfied the values of Ω, Ψ and Λ are changing by an insignificant amount. Moreover, the sensitive parameters (*e.g.* separation location, pressure recovery coefficient *etc.*) also show insignificant changes if the iteration is continued further.

When the Reynolds number was large and the inlet swirl or diffuser angle were also large, the convergence criterion could not always be satisfied. For the inlet swirl profile 5, convergence was most difficult for $R \geqq 1500$. Contour plots of the unconverged solutions show a very

unsteady looking behaviour. This may be due to a numerical instability or because the flow in reality is becoming time dependent. It should be noted that solving the equations by S.O.R. is equivalent to following the flow development through a distorted time. Convergence difficulties may therefore be due to time-dependent behaviour.

7. Conclusions

It is not possible to compare the present results directly with those of experiment since experiments are usually concerned with high Reynolds number turbulent flows. For laminar flows, separation occurs much more easily than for turbulent flows. Furthermore, Reynolds number has little effect on performance and flow regime for turbulent flows with $R > 10^4$, but for laminar flows Reynolds number effects are all important. However, trends observed in experimental studies have been predicted in the present work. This is particularly so of the swirl investigations.

Three relevant experimental investigations involving swirling flows in diffusers are known to the authors. The first two are for conical diffusers and the third for an annular diffuser similar to the configurations considered in the present work.

(i) *So* [7] investigates vortex phenomena in a conical diffuser. With certain swirl conditions he observed vortex breakdown with reverse flows at the axis. His flow visualization shows a stagnation bubble that moves towards the inlet with increasing swirl.

(ii) *McDonald, Fox and Van Dewoestine* [11] consider the effects of inlet swirl on pressure recovery and performance for conical diffusers. They found that for badly stalled diffusers, the introduction of inlet swirl improves performance. They also observed that for a given situation, there is a definite optimum inlet swirl and that the use of very large inlet swirl can be highly detrimental to the flow.

(iii) *Hoadley* [10] examines the effects of swirl in an annular diffuser almost identical to the one considered in the present study. As previously mentioned, it is from this work that some of the inlet profiles of fig. 1 are taken. Hoadley observed separation on the outer casing for zero swirl and on the hub for high inlet swirl. He states that for the largest inlet swirl profile the region of separation at the hub extends nearly to the diffuser inlet. The flow actually reattaches near the diffuser exit but this is due to the presence of the converging exit section of his apparatus. A sharp decrease in pressure recovery for high inlet swirls is also recorded.

Similar trends have been observed in all three studies and the present work predicts similar behaviour. The qualitative agreement of the present results with [10] is highly encouraging and it is hoped that the extension of the present method by including a suitable turbulence model may provide quantitative agreement. If this were possible, it would provide the diffuser designer with a most powerful tool.

Finally it is worth recording the main features predicted by the present laminar study.

(i) Reynolds number has a significant effect. At low R, no separation occurs and a pressure head at inlet is required to drive the flow. For high Reynolds numbers, viscous effects are smaller and some of the kinetic energy lost is recovered as pressure energy. Separation limits the amount of pressure recovery possible.

(ii) When viscous effects are large and a substantial pressure gradient required to drive the flow, the radial velocity profile at exit is almost identical to that of fully developed pipe annulus flow.

(iii) The effects of inlet swirl are most significant. Small amounts of swirl can reduce separation at the outer casing and improve performance. Large inlet swirl results in a very low pressure region at the hub and separation takes place. Separation of this kind is most detrimental to pressure recovery.

(iv) Swirl induced by hub rotation causes slightly earlier separation but the results are not very significant.

(v) Diffuser angle has a very large effect on performance and flow régime.

(vi) Diffuser length has a minimal effect on the upstream flow with the present boundary conditions.

REFERENCES

[1] C. M. Crane and D. M. Burley, Numerical studies for viscous swirling flow through annular diffusers, Part I: Method, *Journ. of Eng. Math.*, 8 (1974)

[2] G. Sovran and E. Klomp, Experimentally determined optimum geometries for rectilinear diffusers with rectangular, conical or annular cross-section, *Fluid Mechanics of Internal Flow*, Elsevier (1969) 270–319.

[3] S. J. Kline, D. E. Abbott and R. W. Fox, Optimum design of straight walled diffusers, *J. Basic Eng.*, 81 (1959) 321–329.

[4] S. Wolf and J. P. Johnston, Effects of non-uniform inlet velocity profiles on flow regimes and performance in two-dimensional diffusers, *J. Basic Eng.*, 91 (1969) 462–474.

[5] A. M. Binnie, Experiments on the slow swirling flow of a viscous liquid through a tube, *Quart. J. Mech. Appl. Math.*, 10 (1957) 276–290.

[6] J. K. Harvey, Some observations of the vortex breakdown phenomenon, *J. Fluid Mech.*, 14 (1962) 585–592.

[7] K. L. So, Vortex phenomena in a conical diffuser, *AIAA Journal*, 5 (1967) 1072–1078.

[8] Z. Lavan, H. Nielsen and A. A. Fejer, Separation and flow reversal in swirling flows in circular ducts, *The Physics of Fluids* 12 (1969) 1747–1757.

[9] C. M. Crane, *Numerical solution of the Navier–Stokes equations with particular reference to the effects of swirl*, Ph.D. Thesis, The University of Sheffield (1972).

[10] D. Hoadley, *Some measurements of swirling flow in an annular diffuser*, Report W/M(3E) p. 1621 M. E. L. Whetstone, English Electric Co. Ltd. (1970).

[11] A. T. McDonald, R. W. Fox and R. V. Van Dewoestine, *Effects of swirling inlet flow on pressure recovery in conical diffusers*, AIAA paper no. 71–84 (1971) 1–9.

[12] E. C. Maskell, *Flow separation in three dimensions*, Royal Aircraft Establishment, Farnborough, Rept. Aero. 2565 (1955).

[13] R. C. Dean, *Separation and stall, Handbook of Fluid Dynamics*, McGraw Hill (1961) 11.1–11.40.

[14] C. M. Crane, Contour plotting for functions specified at nodal points of an irregular mesh based on an arbitrary two parameter co-ordinate system, *The Computer Journal*, 15 (1972) 382–384.